

Nutation Sequences for Magnetic Resonance Imaging in Solids

H. M. Cho, C. J. Lee, D. N. Shykind, and D. P. Weitekamp

Department of Chemistry, University of California, Berkeley, California 94720, and Materials and Molecular Research Division, Lawrence Berkeley Laboratory, Berkeley, California 94720

(Received 15 July 1985)

Novel radio-frequency NMR pulse sequences are presented and their application to imaging of solids with use of rf field gradients is discussed. The sequences cause a nuclear spin to precess about the static field direction at a rate proportional to the strength of certain of the pulses. This forced precession is independent of the resonance offset and of couplings to other spins. The pulse-sequence design is described by means of coherent averaging theory and is confirmed experimentally and numerically.

PACS numbers: 76.60.-k, 81.70.+r

Imaging of the spatial distribution of nuclear spins by the recording of their magnetic resonance signals in field gradients is a well-known concept with a growing body of applications, particularly in medicine.^{1,2} The central idea is that the linear dependence of the frequency of spin precession on the magnetic field at the nucleus can be converted to a measurement of position along a known field gradient.¹ Nearly all NMR imaging has been done on liquids at resolutions of 10^{-3} – 10^{-1} cm, but the large linewidths in solid samples preclude the direct extension of liquid-state imaging methods to solids. The excellent chemical, orientational, and motional specificity of solid-state NMR, as well as its noninvasive, penetrating nature, suggests that NMR imaging methods applicable to solids^{3–10} would be valuable as well, for example, in materials science.

This Letter introduces a new approach to NMR imaging suitable for solids. A radio-frequency (rf) pulse sequence is described which suppresses dipolar (homonuclear and heteronuclear) and chemical-shift contributions to the linewidth. In addition, the sequence results in a frequency shift of the narrowed line position proportional to the rf field strength of certain of the pulses. Given the line narrowing and the linear dependence of line position on rf field amplitude, a coil capable of producing a switched rf field gradient could be used to achieve spatial discrimination of nuclear spins by observing their forced precession frequency in analogy to a related liquid-state experiment.¹¹ Here we demonstrate the solid-state pulse sequences with a homogeneous coil by varying the pulse nutation angle and observing the predicted linear variation in the position of the narrowed line.

In order to resolve two points in the spin distribution separated by a distance Δr , a gradient of magnitude $G \geq M_2^{1/2}/\Delta r$ is required, where $M_2^{1/2}$ is the square root of the second moment of the presumably unresolved solid-state NMR spectrum. A typical value for protons in a solid would be $G \geq 50$ mT/cm ($M_2^{1/2} = 0.5$ mT, $\Delta r = 10^{-2}$ cm). Rapid switching of

the amplitude and direction of a gradient of this size within the bore of a high-field magnet is impractical. A time-domain view of this inequality is that the precession in the field gradient must last long enough to create a significant difference in phase angle between the magnetization from adjacent picture elements, but that during this time the decay of the magnetization at each point should be minimal. Imaging has been demonstrated without meeting this condition,⁹ but only at the cost of a large loss in signal energy. In applications this would lead to unacceptably long acquisition times and so line narrowing is needed.

The principal contribution to $M_2^{1/2}$ for spin- $\frac{1}{2}$ nuclei in solids is the direct dipolar coupling to nearby spins. Three general approaches have been demonstrated previously which address this fact to achieve NMR imaging of solids with field gradients of less than a millitesla per centimeter. The first^{3,4,10} is to use multiple-pulse line-narrowing techniques^{12–17} or related modulation schemes⁵ to effectively eliminate homonuclear dipolar couplings. The second⁶ is to use the high-order multiple-quantum spectra obtainable in solids to increase the line separation due to the applied gradient by a factor n equal to the number of Larmor-frequency quanta characterizing the observed spectrum. The third⁷ is to observe a dilute spin- $\frac{1}{2}$ isotope (^{13}C), whose spectrum is narrowed by heteronuclear decoupling of the neighboring protons.

The second-largest contribution to the spectral width $M_2^{1/2}$ is the distribution of chemical shifts. This distribution is typically greater in solids than in fluids because of the anisotropic part of the shift tensor. Since the chemical-shift range increases linearly with magnetic field, it is a particularly severe impediment to imaging at a high Larmor frequency, which is otherwise desirable to maximize the signal-to-noise ratio. Two general approaches have been suggested for separating the distribution of chemical shifts from the spatial distribution of nuclear spins in solids. The simplest method¹⁸ is to vary systematically the strength of the field gradient either within⁷ or between^{9,10} pulse se-

quences. This provides a data set from which the chemical shift and spatial distributions can be deconvolved. The price paid is a lower signal energy and a longer data acquisition time. This is a poor bargain when the chemical-shift distribution is unresolved because of powder broadening, chemical complexity, or poor field homogeneity as is typically the case for abundant spins in disordered solids. The second approach,⁴ which has not to our knowledge been experimentally demonstrated, combines multiple-pulse line narrowing with pulsed dc field gradients in between the rf pulses. The phase of the rf and sign of the dc can be chosen in such a way that, over a cycle of several pulses, evolution due to the chemical shifts vanishes, but that due to the gradient accumulates. The gradient switching time of $\leq 10^{-6}$ s required for this scheme is a significant barrier to its experimental implementation. The coils needed to produce a pulsed dc field excite long-lived eddy currents in nearby conductors and couple to the gradient coils used to shim the static field. These problems are minimal with rf gradients.¹¹

The approach of the present work provides the necessary line narrowing while circumventing the need for any dc field gradients. As in the proposal of Mansfield and Grannell,⁴ we begin with a cycle of rf $\pi/2$ pulses whose net effect is to eliminate any evolution of the transverse magnetization due to the rotating-frame spin Hamiltonian. This sequence [Fig. 1(a)] consists of sixteen Larmor-frequency pulses alternating with delays or "windows" and has already appeared as part of a heteronuclear sequence in another context.¹⁹ The first cycle is preceded by a $\pi/2$ pulse to create transverse magnetization and the resulting signal is sampled at the beginning of each cycle with a phase-sensitive quadrature detector. The Fourier transform of this signal is a single line at the spectrometer carrier frequency. This is the zero point of the rotating-frame frequency scale. Such an experimental result on the

protons of adamantane²⁰ at a Larmor frequency of 180 MHz is shown in Fig. 2(a). The experimental width of 64 Hz shows that the 12-kHz dipolar width of the usual solid-state spectrum has been eliminated. Figure 3(a) shows the result of a numerical simulation on a system of three dipolar-coupled spins $\frac{1}{2}$ with three distinct chemical shifts and confirms the effectiveness of the sequence even when both types of interactions are present.

With all internal magnetic interactions eliminated, the next step is to introduce an externally variable field in such a way that the line frequency does depend on it. In order for any such field to have a lowest-order effect on the rapidly toggling magnetization, it too must have a related time dependence. We avoid the technical difficulty of pulsing the dc field by instead modifying the rf field. Figure 1(b) shows an rf sequence which, when superimposed coherently on the sequence in (a), causes an apparent precession around the static-field direction at a frequency proportional to its pulse angle θ . The experimental confirmation of this effect is shown in Fig. 2, where θ ranges from 0° to 17° with proportional changes in the line position. The sequences of Figs. 1(a) and 1(b) were in effect combined into a single sixteen-pulse sequence in a homogeneous coil by use of pulse angles of $\beta_0 \pm \theta$ at those eight points in time where pulses of the two sequences are coincident. Figure 3 shows the corresponding set of numerical simulations on the system with chemical shifts.

The significance of these results for NMR imaging of solids is that elimination of the dipolar and Zeeman interactions has been achieved in a sequence which gives a line position proportional to a continuously variable rf field strength. For imaging, the line-narrowing sequence [Fig. 1(a)] would be delivered by the homogeneous coil, and the line-positioning sequence [Fig. 1(b)] would be delivered synchronously by a rf coil whose field varied linearly across the sam-

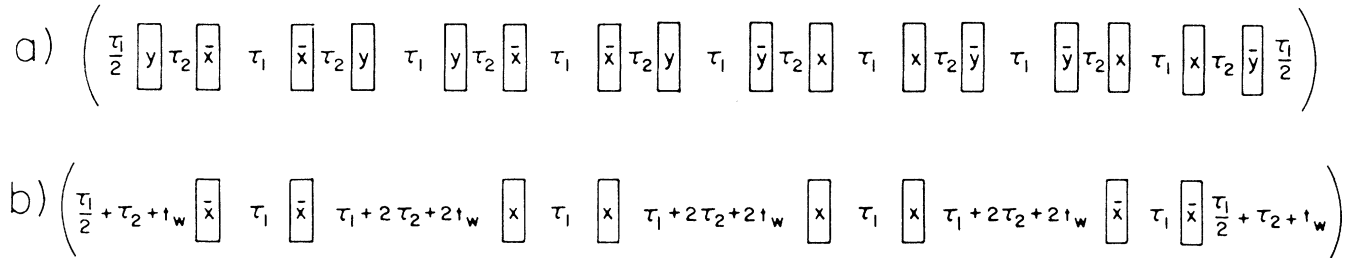


FIG. 1. Nutation sequences for magnetic resonance imaging. The labels x , y , \bar{x} , and \bar{y} indicate four quadrature rf phases. The line-narrowing cycle in (a) eliminates evolution due to both the internal spin Hamiltonian and resonance offsets. The pulse length t_w , pulse angle $\beta_0 \approx \pi/2$, and window lengths τ_1 and τ_2 are optimized as for the WHH-4 sequence (Ref. 16, Sec. 3.5). The sequence in (b) runs synchronously and coherently with that in (a) and forces a net precession of the magnetization through an angle 8θ , where θ is the pulse-angle magnitude for each of the pulses in (b). For NMR imaging, the sequence in (b) is delivered by a rf field-gradient coil, such that θ (and thus the rate of precession) varies linearly across the sample.

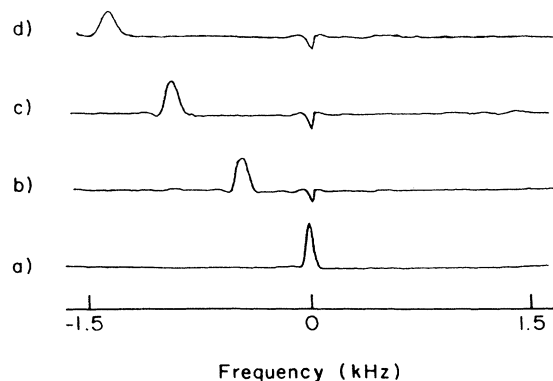


FIG. 2. Experimental demonstration of line narrowing with nutation. The sequences of Figs. 1(a) and 1(b) were superimposed in a single coil by use of pulse angles of $\beta_0 + \theta$ or $\beta_0 - \theta$ depending on whether the phase in (b) is equal or opposite to that of the simultaneous pulse in (a). In this way the concept could be tested with a single probe circuit, amplifier, and pulse-sequence generator. The spectra shown are Fourier transforms of the resulting complex rotating-frame signals. The variation from $\theta = 0^\circ$ in (a) to $\theta = 17^\circ$ in (d) was obtained by variation of pulse length around the value $\beta_0 = 93^\circ$ appropriate to the parameters $t_w = 2.7 \mu\text{s}$, $\tau_1 = 10 \mu\text{s}$, and $\tau_2 = 22.7 \mu\text{s}$. The linear variation in line position with θ confirms the analysis of Eq. (1). The effectiveness of line narrowing over the entire spectral width confirms the possibility of obtaining many resolved picture elements in an imaging experiment where frequency is proportional to spatial position in a gradient of θ . The absence of an image line at positive frequency shows that precession is confined to the transverse plane. Thus the imaging gradient may pass from negative to positive field values within the sample without introducing any ambiguity with respect to signs.

ple. The spins would respond to the coherent superposition of the two applied sequences and thus the value of θ would label a particular plane perpendicular to the gradient.

The pulse-sequence design process can be described with use of a coherent averaging theory by treating the pulses responsible for the precession [Fig. 1(b)] as a perturbation on the sequences of Fig. 1(a), in analogy to the standard treatment¹⁴ of uncontrolled pulse-angle errors. As an example, consider a nutation sequence consisting of pulses of angle θ_i coincident with the i th pulse of Fig. 1(a) and having the same phase. (More general timing and phases are possible, but will not be considered here for simplicity.) The average Hamiltonian for this sequence of total length t_c is

$$\mathcal{H}^{(0)} = (1/t_c)(\kappa_y I_y + \kappa_z I_z), \quad (1)$$

where

$$\kappa_y = \theta_1 - \theta_4 - \theta_5 + \theta_8 - \theta_9 + \theta_{12} + \theta_{13} - \theta_{16}$$

and

$$\kappa_z = \theta_2 + \theta_3 - \theta_6 - \theta_7 + \theta_{10} + \theta_{11} - \theta_{14} - \theta_{15}.$$

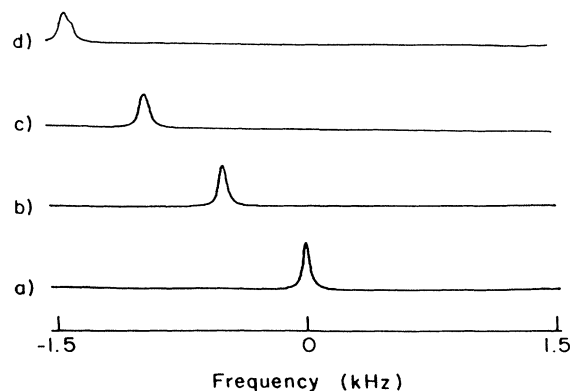


FIG. 3. Computer simulation of line narrowing with nutation on three coupled spins. The pulse timing and strengths are the same as in the corresponding traces of Fig. 2. For each value of θ , the evolution of the transverse magnetization was calculated for 500 repetitions of the sequences in Figs. 1(a) and 1(b) and then multiplied by an exponential decay corresponding to the experimental linewidth found for $\theta = 0$ in Fig. 2(a). The additional θ -dependent linewidth observed in Fig. 2 is also seen in the simulation, indicating that it is intrinsic to the sequence and not due to experimental misadjustment. The dipolar couplings $D_{12} = 3 \text{ kHz}$, $D_{23} = 2 \text{ kHz}$, and $D_{31} = 1 \text{ kHz}$ were chosen to give a spectral width similar to that of adamantane. Chemical shifts of $\nu_1 = -500 \text{ Hz}$, $\nu_2 = 100 \text{ Hz}$, and $\nu_3 = 400 \text{ Hz}$ were added to demonstrate the effectiveness of the sequence in eliminating this source of spectral width.

Although resonance-offset and chemical-shift terms have been eliminated, note that some of the pulse angles now appear as coefficients of the longitudinal component I_z of spin angular momentum. To obtain the sequence of Fig. 1(b), these are set equal in magnitude ($|\theta_i| = \theta$) and their signs (i.e., phases) are chosen to maximize the magnitude of the coefficient of I_z . The result is an apparent resonance-offset frequency of $8\theta/t_c \text{ rad/s}$. Effective transverse fields due to intentional pulse missets [analogous to the I_y term of Eq. (1)] have been used recently for spin locking.¹⁷

The analysis of Eq. (1) suffices to explain the θ -dependent line positions in Figs. 2 and 3. To understand why such large angles can be treated perturbatively is more difficult. One approach is to calculate higher order correction terms¹³⁻¹⁶ $\mathcal{H}^{(n)}$ for the superimposed pulse sequence. The largest possible θ -dependent correction term is the cross term between the nutation pulses and the dipolar couplings. As can be shown analytically, this term is zero for the sequences used. This is confirmed by the fact that the experimental linewidth in Fig. 2 increases only slightly with θ . No attempt has been made to calculate the algebraic form of the underlying correction terms actually responsible for this weak θ dependence. It is of interest, however, that the exact numerical simulation

of Fig. 3 (on a three-spin system with dipolar couplings similar in size to those of adamantane) accurately reproduces the weak θ -dependent line broadening. This indicates the potential of such simulations as an adjunct to algebraic methods in evaluating new pulse sequences.

From the viewpoint of an imaging experiment, this line broadening represents a decrease in resolution toward the edges of the picture. Nevertheless, the resolution achieved suggests that images with ≥ 50 picture elements in each spatial dimension are attainable. The other imperfection is the small line at $\omega = 0$ in Fig. 2, even when $\theta \neq 0$. This corresponds to a bright spot at the center of the image and an effective degradation of that one picture element. This feature was not found in the numerical simulation of Fig. 3, which was performed with square pulses. One possibility is that it arises from the finite rise and fall time ($\sim 3 \times 10^{-7}$ s) of the actual pulses.

An important requirement for sequences designed for high-field imaging of protons is that they perform satisfactorily over the ~ 10 -ppm range of chemical shifts which characterize most solids. Results indistinguishable from Fig. 2 are found in a range of 2 kHz about exact resonance, indicating that an adequate bandwidth has been achieved.

The concept introduced here in one-dimensional form will be most useful when incorporated into multidimensional experiments. Since the dynamics is reduced to that of a two-level system with arbitrary linearly varying or spatially homogeneous coefficients for the transverse and longitudinal terms [Eq. (1)], imaging procedures such as "slice selection"² and Fourier zeugmatography,¹⁸ which were designed for liquids, are now possible in solids. The spatial information from the imaging dimension(s) may also be correlated with spectroscopic information by Fourier transformation with respect to an additional dimension where some part of the internal Hamiltonian is allowed to act in high field or zero field.²¹ Such spectroscopic applications still allow the imaging of such properties as chemical identity, molecular structure, diffusion, restricted motion, reactivity, or spatial orientation. The improvement of these sequences and their incorporation into multidimensional imaging spectroscopy of solids is currently under way.

The authors thank Professor A. Pines for his support and interest in this work. We also thank G. C. Chingas, A. N. Garroway, and N. M. Szeverenyi for

stimulating discussions of their work prior to publication. This work was supported by the Director, Office of Energy Research, Office of Basic Energy Sciences, Materials Science Division of the U. S. Department of Energy and by the Director's Program Development Funds of the Lawrence Berkeley Laboratory under Contract No. DE-AC03-76SF00098.

¹P. C. Lauterbur, *Nature* **242**, 190 (1973).

²P. Mansfield and P. G. Morris, *NMR Imaging in Biomedicine* (Academic, New York, 1982).

³P. Mansfield, P. K. Grannell, A. N. Garroway, and D. C. Stalker, in *Pulsed Nuclear Magnetic Resonance and Spin Dynamics*, Proceedings of the First Specialized Colloque Ampère, edited by J. W. Hennell (Institute of Nuclear Physics, Krakow, Poland, 1973), p. 16.

⁴P. Mansfield and P. K. Grannell, *Phys. Rev. B* **12**, 3618 (1975).

⁵R. A. Wind and C. S. Yannoni, *J. Magn. Reson.* **36**, 269 (1979).

⁶A. N. Garroway, J. Baum, M. G. Munowitz, and A. Pines, *J. Magn. Reson.* **60**, 337 (1984).

⁷N. M. Szeverenyi and G. E. Maciel, *J. Magn. Reson.* **60**, 460 (1984).

⁸B. H. Suits and D. White, *Solid State Commun.* **50**, 291 (1984).

⁹S. Emdin and J. H. N. Creighton, *Physica (Amsterdam)* **128B**, 81 (1985).

¹⁰G. C. Chingas, J. B. Miller, and A. N. Garroway, in Abstracts of the 26th Experimental NMR Conference, Asilomar, California, 1985 (unpublished).

¹¹D. I. Hoult, *J. Magn. Reson.* **33**, 183 (1979).

¹²J. S. Waugh, L. M. Huber, and U. Haeberlen, *Phys. Rev. Lett.* **20**, 180 (1968).

¹³U. Haeberlen and J. S. Waugh, *Phys. Rev.* **175**, 453 (1968).

¹⁴W. K. Rhim, D. D. Elleman, L. B. Schreiber, and R. W. Vaughan, *J. Chem. Phys.* **60**, 4595 (1974).

¹⁵U. Haeberlen, *High Resolution NMR in Solids; Selective Averaging* (Academic, New York, 1976).

¹⁶M. Mehring, *High Resolution NMR Spectroscopy in Solids* (Springer-Verlag, Berlin, 1983).

¹⁷L. Quiroga and J. Virlet, *J. Chem. Phys.* **81**, 4774 (1984).

¹⁸A. Kumar, D. Welti, and R. R. Ernst, *J. Magn. Reson.* **18**, 69 (1975).

¹⁹D. P. Weitekamp, J. R. Garbow, and A. Pines, *J. Chem. Phys.* **77**, 2870 (1982), and **80**, 1372 (1984).

²⁰H. A. Resing, *Mol. Cryst. Liq. Cryst.* **9**, 101 (1969).

²¹D. P. Weitekamp, A. Bielecki, D. Zax, K. Zilm, and A. Pines, *Phys. Rev. Lett.* **50**, 1807 (1983).